

Encapsulation of Lead Sulphide in SBA-15 Molecular Sieve

QING-ZHOU ZHAI*, ZHI-KUN XU and YU XUE

Research Center for Nanotechnology, Changchun University of
Science and Technology, Changchun 130022, P.R. China

Fax: (86)(431)85383815; Tel: (86)(431)85583118

E-mail: zhaiqingzhou@163.com; zhaiqingzhou@hotmail.com

The nanosized channels of SBA-15 molecular sieve were used as template and nanosized lead sulfide was prepared inside them. Pb^{2+} was firstly incorporated into the SBA-15 by ion-exchange method, then the nanosized PbS was prepared in the channels of the SBA-15 molecular sieve using thioacetamide as sulfur source. The (SBA-15)-PbS composite materials were characterized by chemical analysis, powder X-ray diffraction, Fourier transform infrared spectroscopy, low-temperature nitrogen adsorption-desorption technique at 77 K, solid state diffuse reflection absorption spectroscopy and luminescence studies. The PbS has been successfully incorporated in the channels of the SBA-15 molecular sieve and the framework of the SBA-15 in the prepared composite material was kept intact. The prepared host-guest composite material presents luminescence performance and the materials may be hopefully applied to the field of optical materials.

Key Words: Composite material, SBA-15 molecular sieve, Lead sulfide.

INTRODUCTION

Molecular sieve is a kind of material with selective adsorption property and this makes it have a broad prospect in some fields such as chemical, oil, fine chemicals, catalysts, *etc.* As the molecular sieve has the channels of uniform nanosized distribution, this makes the molecular sieve be able used as templates to assemble some materials with optical, electric or magnetic properties. Mesoporous SBA-15 molecular sieve was synthesized in acidic medium by using triblock copolymers poly(1,2-ethylene glycol)-block-poly(propylene glycol)-block-poly(1,2-ethylene glycol) as template¹. It is a mesoporous silica material with highly ordered hexagonal arranged channels, adjustable pore size (4.6-30 nm) and thick silica wall of 3.1-6.0 nm. The thermal stability of SBA-15 is higher than 900 °C, having very high hydrothermal and thermal stability. SBA-15 has opened up a new era of mesoporous materials and arose the scientist's enormous interest. It has the following outstanding features *i.e.*, easy synthesis, the highly ordered hexagonal channels, very narrow pore size distribution, large channel size, large surface area and pore volume, rich surface chemical properties. In recent years, the studies of incorporation of some guests

into the mesoporous channels of molecular sieves have been of great interests and a number of researches have focused on the incorporation of semiconductors including oxides, sulfides, *etc.*². The commonly used methods of preparing host-guest materials include injection method, solid-phase diffusion method, liquid-phase grafting method, ion exchange and co-melting method²⁻⁴. Some rare earth elements can be incorporated into SBA-15 molecular sieve by the ion-exchange of rare earths such as LaCl₃⁴, Ag⁵, Eu⁶, Au⁷, Co-Pb⁸ and other metals have already been incorporated into SBA-15 molecular sieve by ion-exchange method. Zhang *et al.*⁹ prepared Pt nanoclusters in SBA-15 by *in situ* reduction of Si-H bond. Meynen *et al.*¹⁰ prepared SBA-15-vanadium silicalite-1 by injection method. Wang *et al.*¹¹ prepared Fe in SBA-15, enhancing the thermal stability of the molecular sieve and catalytic capacity. Optical properties of nano-semiconductor correspond closely to its size. Thus, precisely controlling its size and size distribution is of interest. In recent years, mesoporous materials as host to restrict the growth of semiconductor nanomaterials in their channels became an important research direction. Some semiconductor nanomaterials such as CdSe¹², ZnS^{13,14} have been successfully assembled in the MCM-41 molecular sieves and TiO₂¹⁵, ZnO¹⁶ in the SBA-15 silica. As II - VI semiconductor material, PbS has a narrow band gap (0.41 eV). However, the band gap of nanoscale PbS will increase from near infrared to the visible blue region, showing a unique optical properties¹⁷. Thus it has broad prospects in applications of nonlinear optical devices, infrared detectors, display devices, light emitting diodes, single electron transistors, field-effect thin-film transistors, photoelectric conversion materials. Therefore, incorporating PbS into mesoporous materials attracted great interest. For the preparation of this kind of materials, ion exchange method is generally used to introduce metal ions into the molecular sieve and then a toxic substance H₂S was used as a source of sulfur to prepare sulfide inside the molecular sieves¹⁸. However, H₂S is toxic and is not convenient for operation. Gao *et al.*¹⁹ reported the preparation of PbS inside SBA-15 using functionalization of the channel surfaces with thiol groups, absorption of Pb²⁺ and heating in N₂ atmosphere at high temperature. However, the operation of this preparative method was complicated. In this work, SBA-15 molecular sieve is selected as host and (SBA-15)-Pb sample was firstly prepared by ion exchange and then (SBA-15)-PbS composite materials were prepared using thioacetamide as sulfur source. A safe and feasible way was used to prepare the host-guest material by using thioacetamide precursor as sulfur source, avoiding the inconvenience and toxicity of directly using H₂S¹⁸. The samples were characterized by means of chemical analysis, powder X-ray diffraction, infrared spectroscopy, low temperature nitrogen adsorption-desorption technique at 77 K, solid state diffuse reflection absorption spectroscopy and luminescence studies. The composite materials (SBA-15)-PbS prepared have potential application prospect in the fields of optical materials. Compared with the previous work^{18,19}, the present procedure is easy to be operate.

EXPERIMENTAL

Amphiphilic triblock copolymer, poly(ethylene glycol)-block-poly(propylene glycol)-block-poly(ethylene glycol) (Fluka); tetraethyl orthosilicate (TEOS, Shanghai Chemical Co. Ltd., China); hydrochloric acid (Beijing Chemical Plant, China); lead acetate (Shanghai Chemical Corporation of Chinese Medicine Group, China); thiacetamide (Shanghai Lingfeng Chemical Co. Ltd., China); deionized water. All reagents used were of analytical grade unless specifically stated.

Preparative method of (SBA-15)-PbS Host-Guest composite material

Preparation of host material SBA-15 molecular sieve: 2 g of triblock copolymer poly(1,2-ethylene glycol)-block-poly(propylene glycol)-block-poly(1,2-ethylene glycol) (Template, T) was dissolved in 60 g of 2 mol L⁻¹ hydrochloric acid solution and 15 g of deionized water, stirring until completely dissolved then 4.25 g tetraethyl orthosilicate (TEOS) was added dropwise add to form a homogeneous solution. The initial molar ratio of material was T:TEOS:HCl:H₂O = 1:59:348:2417. This mixed solution was stirring for 24 h at 40 °C. Then at the temperature of 100 °C the solution was crystallized in a Teflon-lined autoclave for 48 h. The obtained sample was filtrated, watered with deionized water, dried at room temperature and then calcined at 550 °C for 24 h in air to remove the triblock copolymer. Then host material SBA-15 molecular sieve white powder was obtained.

Preparation of (SBA-15)-PbS host-guest composite: Firstly, 0.8000 g of the SBA-15 was added to 80 mL of 0.10 mol L⁻¹ lead acetate solution, stirred for 48 h, filtered, washed, placed in an oven at 60 °C for drying for 6 h. The above product (SBA-15)-Pb, 0.3808 g of thioacetamide and 80 mL of water were put into a Teflon-lined autoclave and heated in an oven at 80 °C for 48 h. The product was filtered, washed with deionized water, dried at 60 °C for 6 h and then host-guest composite was obtained and designated as (SBA-15)-PbS.

Characterization of samples: Determination of silicon was made by siliconantimomolybdate heteropoly blue photometry²⁰ with a 722S spectrophotometer (Shanghai Lingguang Technology Co., Ltd., China). The content of lead was determined by atomic absorption spectrometry with Hitachi Z-8000 polarization Zeeman atomic absorption spectrophotometer. The content of sulfur was measured by gravimetric method. X-ray diffraction (XRD) patterns were collected with a diffractometer (D5005, Siemens, Germany) with CuK_α ($\lambda = 1.5418 \text{ \AA}$) radiation operated at 30 kV and 20 mA with step size of 0.02°. Fourier transform infrared (FT-IR) spectra were recorded on a Nicolet 5DX-FTIR spectrometer, using the potassium bromide wafer technique. N₂ adsorption-desorption experiments were carried out at 77 K on a Micromeritics ASAP2010M instrument. Before the measurements, the sample was outgassed for at least 12 h at 573 K. The results were calculated with BdB model²¹. The specific surface area and pore size distributions were derived by using BET²² and BJH²³ methods, respectively. Solid state diffuse reflection spectra were recorded with a Cary 500 ultraviolet-visible-near infrared spectrophotometer (Varian, USA). The luminescence studies were performed on SPEX-FL-2T2 (American SPEX Company) double grafting fluorometer.

RESULTS AND DISCUSSION

Chemical analysis: The contents of lead and sulfur in the host-guest composite material (SBA-15)-PbS were obtained by atomic absorption spectrometry and gravimetric method, respectively. The content of silicon in the (SBA-15)-PbS sample was determined by siliconantimomolybdate heteropoly blue photometry²⁰. The content of oxygen was obtained by subtraction method. The results showed that the contents of Pb, S, Si, O in the prepared host-guest composite material were 5.31, 0.82, 43.81 and 50.06 % in mass, respectively and the formula of (SBA-15)-PbS sample was $\text{PbSSi}_{61}\text{O}_{122}$. The chemical analysis showed the presence of the guest PbS in the prepared host-guest composite material.

XRD analysis: Fig. 1 shows the small-angle XRD patterns of the SBA-15, (SBA-15)-Pb and (SBA-15)-PbS. The XRD patterns of three samples show very intense diffraction peaks which are indexed to 100 planes. For the SBA-15 sample (curve A) three peaks with lower intensity at higher degree appear, which are indexed to 110, 200 and 210 planes, indicating that highly ordered SBA-15 has been prepared. The peak intensity in curve (B) and (C) decreases compared with that of curve (A) due to the incorporation of lead and PbS. This shows that the ordering of the SBA-15 in the (SBA-15)-Pb and (SBA-15)-PbS samples decreased. However, the frameworks of the samples were kept intact.

Fourier transform infrared spectra: The infrared spectra of the samples are shown in Fig. 2. Curve (A) and (B) respond to the spectra of SBA-15 and (SBA-15)-

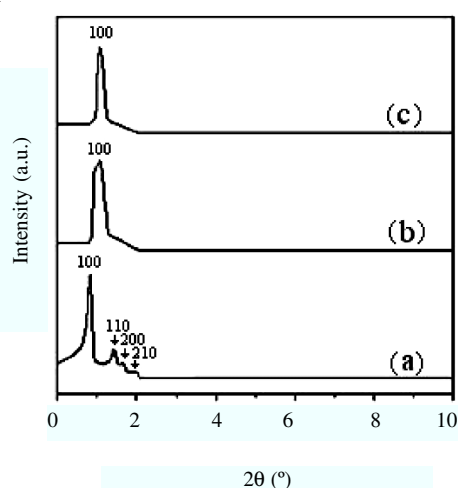


Fig. 1. XRD patterns of the samples: (a) SBA-15; (b) (SBA-15)-Pb; (c) (SBA-15)-PbS

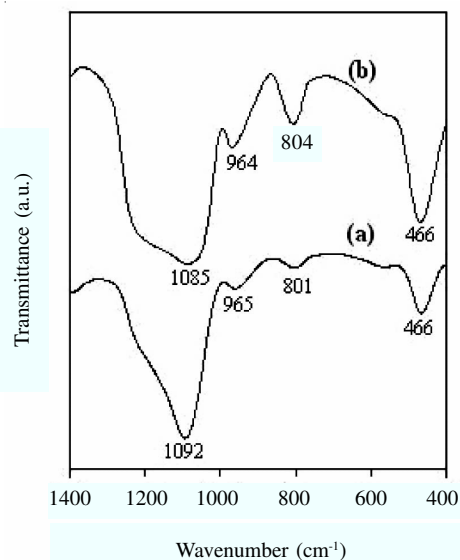


Fig. 2. Infrared spectra of the samples: (a) SBA-15; (b) (SBA-15)-PbS

PbS. Curve (A) shows a peak at 466 cm^{-1} which responds to the bending vibration of the Si-O-Si, the peak at 801 cm^{-1} responds to the symmetric stretching vibration of the Si-O-Si, the peak at 965 cm^{-1} responds to the bending vibration of the Si-OH, the broader peak at 1092 cm^{-1} responds to the asymmetric stretching vibration of the Si-O-Si, respectively. There is not any peak of PbS in the curve of the (SBA-15)-PbS, which indicates that PbS homogeneously dispersed in the channels of the SBA-15.

Low temperature nitrogen adsorption-desorption isotherms and pore distribution: Fig. 3 shows low temperature nitrogen adsorption-desorption isotherms of SBA-15 and (SBA-15)-PbS. Both isotherms can be classified as type IV isotherms, *i.e.* the typical adsorption on the pore surface of cylindrical mesopores and apparent hysteresis loop appear at the higher section of curves. It shows that the curves of SBA-15 and (SBA-15)-PbS are very similar, indicating that PbS did not make the channel structure of the SBA-15 present obvious change. H1 hysteresis loop appears in both curves of the samples, which also proved that PbS nanoparticles dispersed well in mesoporous channels of the molecular sieve. With the increase in loading of PbS, its BET surface area and pore volume evenly decreased. For the SBA-15 sample, the curve is smooth at the relative pressure of $P/P_0 < 0.67$ due to monolayer adsorption of nitrogen molecules in the pore. At the relative pressure of $0.67 < P/P_0 < 0.85$, N_2 adsorption suddenly increases. At the relative pressure of $P/P_0 > 0.85$, the adsorption capacity slowly increases, indicating that adsorption gradually reached saturation. For the (SBA-15)-PbS sample, the curve is smooth at the relative pressure of $P/P_0 < 0.6$, which is due to monolayer adsorption of nitrogen molecules in the pore. At the relative pressure of $0.6 < P/P_0 < 0.87$, N_2 adsorption suddenly increased. At the relative pressure $P/P_0 > 0.87$, the adsorption capacity slowly increased, indicating that adsorption gradually reached saturation. Meanwhile, gas adsorption of the (SBA-15)-PbS has decreased, showing that PbS has been introduced into the ordered channels.

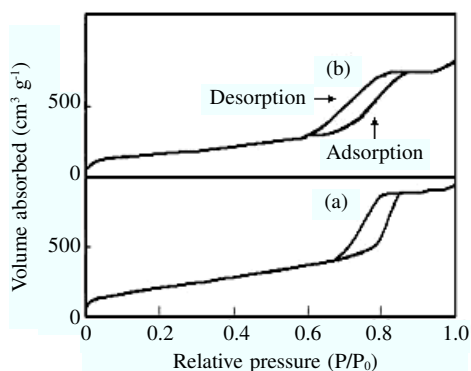


Fig. 3. Low temperature nitrogen adsorption-desorption isotherms of the samples: (a) SBA-15; (b) (SBA-15)-PbS

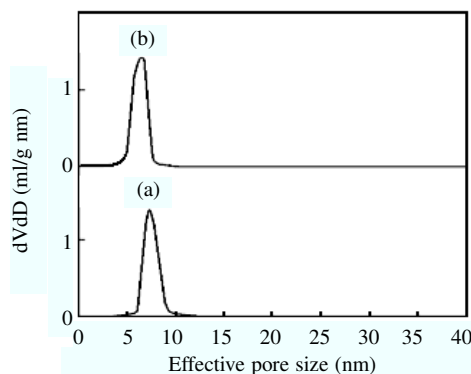


Fig. 4. Pore size distribution patterns of the samples: (a) SBA-15; (b) (SBA-15)-PbS

The pore size distribution curves are shown in Fig. 4. It can be seen that the SBA-15 and (SBA-15)-PbS samples have ordered one-dimensional structure and narrow pore size distribution. The pore size decreased after the incorporation of PbS, showing that PbS located in the channels of the molecular sieve host.

Compared with the SBA-15, the surface area, pore size, pore volume and other parameters of (SBA-15)-PbS are lower and the data are shown in Table-1. This also proves that the internal pore of the mesoporous material SBA-15 was occupied by PbS. PbS has been successfully assembled into the channels of the host SBA-15.

TABLE-1
PORE STRUCTURE PARAMETERS OF THE SAMPLE

Sample	d_{100} (nm)	a_0^a (nm)	BET surface area ($\text{m}^2 \text{g}^{-1}$)	Pore volume ^b ($\text{cm}^3 \text{g}^{-1}$)	Pore size ^c (nm)	Wall thickness ^d (nm)
SBA-15	10.44	12.06	662	1.14	6.77	5.29
(SBA-15)-PbS	8.33	9.62	466	0.93	6.41	3.21

^a $a_0 = \frac{2}{\sqrt{3}} d_{100}$; ^b BJH adsorption cumulative volume of pores; ^c Pore size calculated from the desorption branch; ^d Wall thickness calculated by (a_0 - pore size)

For calculating the blockage effect of PbS on the channels of the SBA-15 molecular sieve quantitatively, in this study the normalized surface area of materials (NSA)²⁴ was calculated. According to the normalized surface area value of material the state of guest in the composite materials can be determined as follows²⁴: (1) When the normalized surface area of composite material is $\ll 1$, the guest material will form relatively larger particles (Fig. 5a). These particles enter the channels of the molecular sieve, blocking the channels, making the pore volume, surface area and pore size of molecular sieve dramatically smaller. (2) When the normalized surface area of composite material is approximately equals to 1, the guest material will form a noncrystal layer, closely covering the inner surface of the molecular sieve (Fig. 5b). Because these particles attached to the inner surface of the molecular sieve form a new surface, it only covers the original surface. Thus, the normalized surface area value of this type is close to 1. (3) When the normalized surface area of composite material is > 1 , the guest material will become very small nanocrystals. It disperses on the internal and external surface of the molecular sieve (Fig. 5c), because the size of these nanocrystals is very small, making a significant increase of surface area in the composite material. So the normalized surface area is much larger than 1.

The formula of normalized surface area (NSA) is as follows²⁴:

$$\text{NSA} = \frac{\text{SA}_1}{1-y} \times \frac{1}{\text{SA}_2}$$

SA_1 and SA_2 are the surface area of (SBA-15)-PbS composite materials and the original SBA-15 molecular sieve powder, respectively, y is mass fraction of the PbS in the composite material.

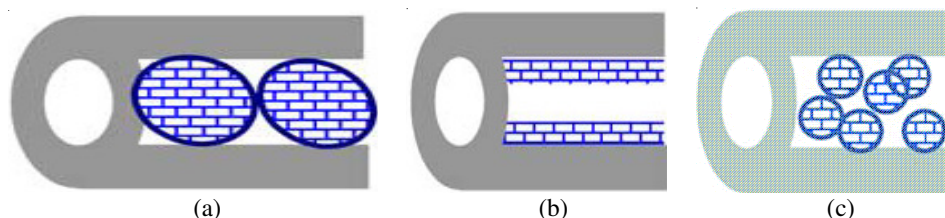


Fig. 5. Guest phase assembling inside the SBA-15: (A) Type I; (B) Type II; (C) Type III²⁴

In the present study, the normalized surface area values of the (SBA-15)-PbS samples is 0.8 from the normalized surface area values of the samples. It is observed that the normalized surface area value of the (SBA-15)-PbS sample is approximately equals to 1. Therefore, PbS materials formed a noncrystal layer in the (SBA-15)-PbS sample. This made pore volume, surface area and pore size of the molecular sieve smaller. These results and the nitrogen adsorption-desorption isotherms results were consistent.

Optical properties

UV-Vis solid state diffuse reflection spectra: The UV-Vis diffuse reflection spectra of the samples shows (Fig. 6) that there is no absorption from SBA-15 (curve A) in the range of the wavelength studied. However, after being incorporated PbS the host-guest composite shows absorption. Absorption peaks are located at 228 and 314 nm. Compared with the bulk PbS (curve B), the absorption of (SBA-15)-PbS (curve C) shows blue-shifts 16 and 14 nm to 244 and 328 nm of the bulk PbS, respectively. Blue shifts took place because the band gap energy increases. This is determined by the confinement effect of channels of the SBA-15 molecular sieve. Meanwhile, this further illustrates that the PbS has been incorporated into the channels of the SBA-15 molecular sieve. The enormous surface area of the SBA-15 provides sufficient space for embedded PbS particles, ensuring the space distance among PbS particles. The results of the UV-Vis diffuse reflection absorption spectra further illustrate that PbS has been successfully assembled into the SBA-15.

Luminescence: The luminescence spectrum of the (SBA-15)-PbS sample is shown in Fig. 7. Semiconductor nanocrystals photoluminescence spectra generally consist of two light-emitting zones. A narrow and weak emission peak locates in a UV region, which comes from transitions between excitation energy levels of band edge, known as the band edge or excitation emission. The other is a wide and strong luminescence band located in a visible region, which is caused by transitions of impurities or defects, known as impurities or defects emission. The emission peak locates at 487 nm (visible range) in this paper. The reason is that the size of PbS is very small, the probability of forming defects on the surface is very high. Thus, the luminescence of the sample was caused by surface defects. SBA-15 itself does not have the property of luminescence, but good luminous performance appears after incorporating PbS. The (SBA-15)-PbS composite material prepared in this paper is expected to be applied as luminescence materials.

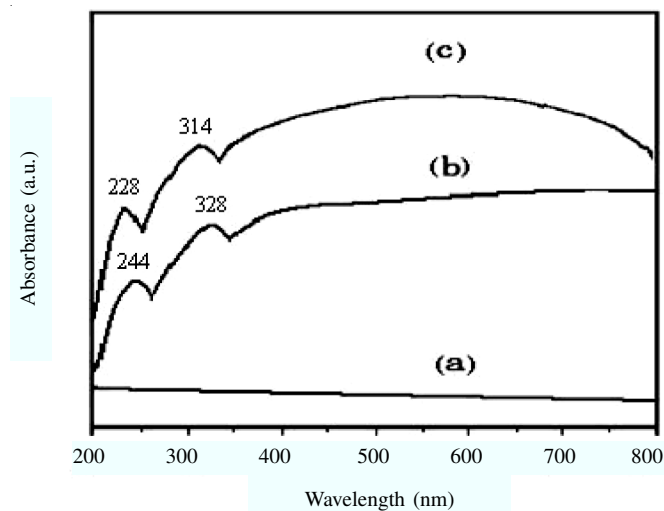


Fig. 6. Solid state diffuse reflection absorption spectra of the samples: (a) SBA-15; (b) PbS; (c) (SBA-15)-PbS

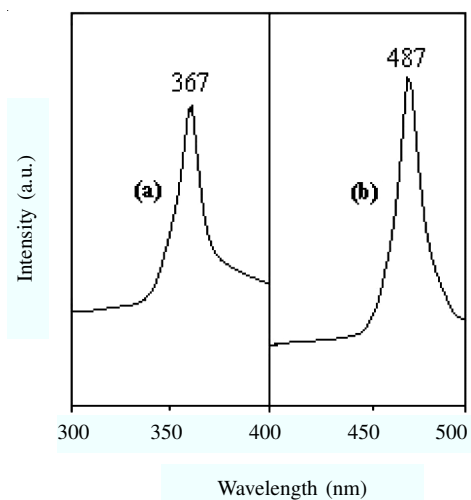


Fig. 7. Luminescence of the (SBA-15)-PbS sample: (a) excitation spectrum ($\lambda_{em} = 487$ nm); (b) emission spectrum ($\lambda_{ex} = 367$ nm)

Conclusion

The composite material (SBA-15)-PbS was prepared and characterized by different techniques. Chemical analysis showed the presence of the guest PbS in the prepared host-guest composite material. Powder X-ray diffraction and FT-IR indicated the structural integrity of the SBA-15 in the (SBA-15)-PbS sample. The low-temperature nitrogen adsorption-desorption at 77 K indicated that the prepared (SBA-15)-PbS sample had mesoporous channels and a narrow pore size distribution and the PbS

had been located in the SBA-15. Solid state diffuse reflection absorption spectra showed the stereoscopic confinement effect of the SBA-15 host channels on the guest PbS and the guest was in the channels of the host. The (SBA-15)-PbS composite material has the promising applied prospect as luminous material.

ACKNOWLEDGEMENT

The authors are grateful to The Department of Science and Technology, Ministry of Education, P. R. China, for the financial support to this research. The grant number was 02044/259606.

REFERENCES

1. D.Y. Zhao, J.L. Feng, Q.S. Huo, N. Melosh, G.H. Fredrickson and B.F. Chmelka, *Science*, **279**, 548 (1998).
2. J.L. Shi, Z.L. Hua and L.X. Zhang, *J. Mater. Chem.*, **14**, 795 (2004).
3. Q.Z. Zhai, Nanotechnology, Beijing: Weapon Industry Press, p. 386 (2006).
4. Q.Z. Zhai and W. Wang, *J. Inorg. Mater.*, **19**, 1212 (2004).
5. L.M. Worboys, P.P. Edwards and P. Anderson, *Chem. Commun.*, **23**, 2894 (2002).
6. C.W. Gu, P.A. Chia and X.S. Zhao, *App. Surf. Sci.*, **237**, 387 (2004).
7. Z. Konya, V.F. Puentes and I. Kiricsi, *Nano. Lett.*, **2**, 907 (2002).
8. C. Mukaddes, A. Burcu, Y. Aysen and U. Deniz, *Turk. J. Phys.*, **29**, 287 (2005).
9. L.X. Zhang, J.L. Shi and J. Yu, *Adv. Mater.*, **14**, 1510 (2002).
10. V. Meynen, P. Cool, E.F. Vansant, P. Kortunov and F. Grinberg, *Micropor. Mesopor. Mater.*, **99**, 14 (2007).
11. X.Q. Wang, H.L. Ge, H.X. Jin and Y.J. Cui, *Micropor. Mesopor. Mater.*, **86**, 335 (2005).
12. H. Parala, H. Winkler, M. Kolbe, A. Wohlfart and R.A. Fischer, *Adv. Mater.*, **12**, 1050 (2000).
13. W.H. Zhang, J.L. Shi, H.R. Chen, Z.L. Hua and D.S. Yan, *Chem. Mater.*, **13**, 648 (2001).
14. C. Weon-Sik, Y. Joong-Ho, Y. Hyunung, D.J. Jang and Y.R. Kim, *J. Phys. Chem. B*, **108**, 11509 (2004).
15. M.V. Landau, L.Vradman and X.G. Wang, *Micropor. Mesopor. Mater.*, **78**, 117 (2005).
16. Q. Jiang, Z.Y. Wu and Y.M. Wang, *J. Mater. Chem.*, **16**, 1536 (2006).
17. L.Z. Yao, C.H. Ye, J.M. Mou and W.L. Cai, *J. Inorg. Mater.*, **16**, 93 (2001).
18. Z.T. Zhang, S. Dai, X.D. Fan, D.A. Blom, S.J. Pennycook and Y. Wei, *J. Phys. Chem. B*, **105**, 6755 (2001).
19. F. Gao, Q.Y. Lu, X.Y. Liu, Y.S. Yan and D.Y. Zhao, *Nano Lett.*, **1**, 743 (2001).
20. Q.Z. Zhai and C.Y. Mei, *Hydrometallurgy (China)*, **4**, 56 (1998).
21. J.C.P. Broekhoff and J.H. Deboer, *J. Catal.*, **10**, 307 (1968).
22. S. Brumauer, P.H. Emmett and E. Teller, *J. Am. Chem. Soc.*, **60**, 309 (1938).
23. E.P. Barrett, L.G. Joyner and P.P. Halenda, *J. Am. Chem. Soc.*, **73**, 373 (1951).
24. L.Vradman, M.V. Landau, D. Kantorovich, Y. Koltypin and A. Gedanken, *Micropor. Mesopor. Mater.*, **79**, 307 (2005).